



HUNGARIAN UNIVERSITY OF AGRICULTURE AND LIFE
SCIENCES

Influence of moisture content on soil bearing capacity
and spectral reflectance

PhD Thesis

by

Ahmed Elawad Eltayeb Ahmed

Gödöllő
2025

Doctoral school

Denomination: Doctoral School of Mechanical Engineering

Science: Mechanical Engineering

Leader: Prof. Dr. Gábor Kalácska, DSc
Institute of Technology
Hungarian University of Agriculture and Life Sciences,
Gödöllő, Hungary

Supervisor: Prof. Dr. Péter Kiss, PhD
Institute of Technology
Hungarian University of Agriculture and Life Sciences,
Gödöllő, Hungary

Co-Supervisor: Dr. György Pillinger, PhD
Institute of Technology
Hungarian University of Agriculture and Life Sciences,
Gödöllő, Hungary

.....
Affirmation of supervisor

.....
Affirmation of head of school

CONTENTS

1. INTRODUCTION, OBJECTIVES	4
2. MATERIALS AND METHODS.....	5
2.1. Soil types and preparation.....	5
2.2. Experimental procedure	6
3.2.1 <i>Load-bearing capacity measurement (bevameter test)</i>	6
3.2.2 <i>Determining the moisture content of the soil</i>	9
3.2.3 <i>Spectral behaviour measurements (colour test)</i>	9
3. RESULTS	10
3.2. The impact of moisture content	11
3.2.1 <i>On the soil density</i>	11
3.2.2 <i>On the soil relative sinkage</i>	11
3.3. Spectral behaviour (Spectrophotometer).....	12
3.3.1 <i>Colour affected by moisture contents</i>	12
3.4. Soil properties underload and the spectral reflectance at 700 nm	15
3.4.1 <i>Soil relative density ratio – reflectance at 700 nm relationship</i>	15
3.4.2 <i>Soil relative sinkage – spectral reflectance at 700 nm relationship</i>	15
3.5. Estimation of soil-specific constants and moisture content	16
3.6. Soil load bearing capacity – optical reflectance relationship.....	16
3.7. Soil saturation- spectral reflectance relationship.....	18
3.8. The effect of the load velocity on the soil sinkage.....	19
4. NEW SCIENTIFIC RESULTS	20
5. CONCLUSION AND SUGGESTIONS	25
6. SUMMARY	26
7. MOST IMPORTANT PUBLICATIONS RELATED TO THE THESIS	27

1. INTRODUCTION, OBJECTIVES

Understanding the substrate on which a vehicle operates is fundamental to land locomotion studies. The mechanical properties of the soil, particularly the load-bearing capacity and shear strength, are critical for predicting its response to vehicle-induced loads. The load-bearing capacity dictates whether the soil can sustain the normal pressure exerted by a wheel without excessive sinkage, whereas the shear strength prevents internal failure and ensures stability during movement. The experimental evaluation of these properties, often conducted using the bevameter technique, provides a foundation for analysing soil deformation and optimising vehicle design and operation in off-road environments.

The soil moisture content significantly influences its mechanical and spectral properties. Increased moisture enhances compaction, alters load-bearing capacity, and modifies spectral behaviour by darkening soil colouration. The correlation between soil colour and mechanical properties presents promising opportunities for off-road engineering applications. Integrating soil colour data into remote sensing technologies makes it possible to assess soil load-bearing capacity in real time, aiding in navigation decisions for autonomous vehicles. Quantitative methods, such as spectrophotometry, provide precise soil colour analysis and enable robust terrain assessments. This study renders the main objectives listed below:

- Investigate to examine the load-bearing capacity of eight varieties of soil with diverse moisture content.
- Additionally, the soil colour (spectral behaviour) for the above-mentioned types of soil with the same diverse moisture content must be identified.
- Determine the relationship between the soil load-bearing capacity and its relative sinkage and relative density ratio and ascertain which one is more suitable.
- Identify the soil colour (spectral behaviour) at various moisture content ranges to determine which range should be considered to evaluate the reflectance behaviour.
- Establish the connection between the soil properties (load-bearing capacity, soil colour) to determine their relationship between them.
- Investigate the spectral reflectance of eight types of soil at zero moisture content (MC = 0.00%) to determine which ones have the highest and lowest reflectance.
- Moreover, investigate the influence of plate size and loading speed on the pressure-sinkage relationship of sandy loam soil.
- Conduct measurements using the cone index (CI) to determine the penetration resistance - depth relationship, as well as the spectral behaviour of the sandy loam soil (field measurement).

2.MATERIAL AND METHODS

2. MATERIALS AND METHODS

This chapter outlines the materials, methods, equipment, and experimental procedures employed to achieve the research objectives.

2.1. Soil types and preparation

Eight different types of soil were collected from various regions in Hungary, as listed in Table 2.1 and depicted in the triangle-textured diagram (Figure 2.1). The soil was sieved through a 5 mm mesh to remove coarse particles and plant roots for studying it as a homogeneous material.

Table 2.1. Shows eight soil textures from different regions in Hungary.

Soil no.	Soil type	Sand (%)	Silt (%)	Clay (%)	Location	Coordinates
1	Sandy loam	90.50	03.20	06.30	Gödöllő, Hungary	47.5816264, 19.3984064
2	Silty loam	11.64	62.18	26.18	Karcag, Hungary	47.2884618, 20.9213624
3	Clay	13.16	31.28	55.56	Karcag, Hungary	47.235285, 20.7345042
4	Sand	95.68	02.12	02.21	Csölyospáros, Hungary	46.3954473, 19.8210738
5	Silty clay	03.34	52.05	44.61	Karcag, Hungary	47.2829123, 20.8821998
6	Clay loam	30.77	40.70	28.53	Sopron, Hungary	47.6924941, 16.635592
7	Loam	31.29	49.67	19.03	Sopron, Hungary	47.6709397, 16.5644485
8	Loamy sand	82.13	12.10	05.77	Órbottyán, Hungary	47.6743804, 19.2466272

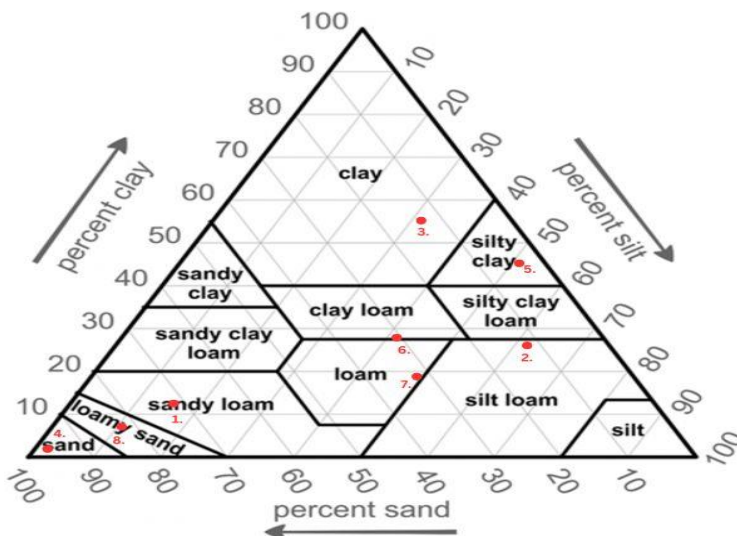


Figure 2.1. Shows the eight soil textures as mentioned in Table 1.

2.2. Experimental procedure

3.2.1 Load-bearing capacity measurement (bevameter test)

In the bevameter experiment (Figure 2.2a), plate penetration was utilised to measure pressure–sinkage parameters (force and displacement, Figure 2.2d) influencing motion resistance. Data acquisition was facilitated by CATMAN 4.5 software via a Spider8 data logger (Figure 2.2c).

Initially, the soil was sieved at ambient moisture conditions (section 2.2) and prepared in a bevameter bin ($H_1 = 12$ cm, $D_1 = 22$ cm). It was filled to $H_2 = 10$ cm and centred beneath a pressing plate ($D_2 = 20$ cm, Figure 2.2b). Two sensors recorded vertical displacement (mm) and applied load (N), with force-displacement data plotted against time (Figure 2.2c, 2.2d).

Tests were conducted under ambient conditions and subsequently repeated with increased moisture content. Following each test, the soil was removed, homogenised with water, and measured for mass and post-compression height (H_3). Initial (ρ_1) and post-compression (ρ_2) densities were calculated by Equation 2.1 and their values were used to determine the relative density ratio ($\Delta\rho$). The fixed H_2/D_2 ratio (0.5) ensured consistency and soil behaviour consistent with infinite-space conditions. Testing parameters for eight soil textures and six moisture levels are summarised in Table 2.2.

$$\rho_{1,2} = \frac{m}{\pi \cdot r^2 \cdot H_{2,3}} \quad (2.1)$$

Table 2.2. shows eight samples of soil with the same density but different moisture content.

Soil type	No.	H2/D2	MC [%]	Mass [kg]	Height [cm]	$\rho_{1,2}$ [g/cm ³]	$\Delta\rho$ [-]
Sandy loam	1	0.5	01.12	4.75	$H_2= 10,$ $H_3= 9.0$	$\rho_1 = 1.51,$ $\rho_2= 1.68$	0.17
	2	0.5	04.68	4.75	$H_2= 10,$ $H_3= 8.1$	$\rho_1 = 1.51,$ $\rho_2= 1.87$	0.35
	3	0.5	08.77	4.75	$H_2= 10,$ $H_3= 7.5$	$\rho_1 = 1.51,$ $\rho_2= 2.02$	0.50
	4	0.5	12.00	4.75	$H_2= 10,$ $H_3= 7.1$	$\rho_1 = 1.51,$ $\rho_2= 2.13$	0.62
	5	0.5	15.04	4.75	$H_2= 10,$ $H_3= 6.9$	$\rho_1 = 1.51,$ $\rho_2= 2.19$	0.68
Silty loam	1	0.5	05.70	3.71	$H_2= 10,$ $H_3= 7.5$	$\rho_1 = 1.18,$ $\rho_2= 1.57$	0.39
	2	0.5	07.91	3.71	$H_2= 10,$ $H_3= 7.3$	$\rho_1 = 1.18,$ $\rho_2= 1.62$	0.44
	3	0.5	11.30	3.71	$H_2= 10,$ $H_3= 6.8$	$\rho_1 = 1.18,$ $\rho_2= 1.74$	0.56
	4	0.5	14.49	3.71	$H_2= 10,$ $H_3= 6.2$	$\rho_1 = 1.18,$ $\rho_2= 1.90$	0.72

2.MATERIAL AND METHODS

	5	0.5	17.56	3.71	$H_2=10,$ $H_3=5.7$	$\rho_1=1.18,$ $\rho_2=2.07$	0.89
Clay	1	0.5	10.23	3.56	$H_2=10,$ $H_3=7.1$	$\rho_1=1.13,$ $\rho_2=1.60$	0.46
	2	0.5	14.40	3.56	$H_2=10,$ $H_3=6.4$	$\rho_1=1.13,$ $\rho_2=1.77$	0.64
	3	0.5	17.00	3.56	$H_2=10,$ $H_3=5.8$	$\rho_1=1.13,$ $\rho_2=1.95$	0.82
	4	0.5	21.58	3.56	$H_2=10,$ $H_3=5.6$	$\rho_1=1.13,$ $\rho_2=2.02$	0.89
	5	0.5	24.19	3.56	$H_2=10,$ $H_3=5.4$	$\rho_1=1.13,$ $\rho_2=2.10$	0.97
	6	0.5	26.73	3.56	$H_2=10,$ $H_3=5.5$	$\rho_1=1.13,$ $\rho_2=2.08$	0.93
Sand	1	0.5	01.09	4.71	$H_2=10,$ $H_3=8.9$	$\rho_1=1.50,$ $\rho_2=1.68$	0.19
	2	0.5	03.90	4.71	$H_2=10,$ $H_3=8.8$	$\rho_1=1.50,$ $\rho_2=1.70$	0.20
	3	0.5	06.74	4.71	$H_2=10,$ $H_3=8.5$	$\rho_1=1.50,$ $\rho_2=1.76$	0.26
	4	0.5	09.37	4.71	$H_2=10,$ $H_3=8.3$	$\rho_1=1.50,$ $\rho_2=1.81$	0.31
	5	0.5	12.19	4.71	$H_2=10,$ $H_3=7.7$	$\rho_1=1.50,$ $\rho_2=1.95$	0.45
	6	0.5	15.08	4.71	$H_2=10,$ $H_3=7.5$	$\rho_1=1.50,$ $\rho_2=2.00$	0.50
Silty clay	1	0.5	04.02	3.00	$H_2=10,$ $H_3=7.6$	$\rho_1=0.95,$ $\rho_2=1.26$	0.30
	2	0.5	10.69	3.00	$H_2=10,$ $H_3=6.4$	$\rho_1=0.95,$ $\rho_2=1.49$	0.54
	3	0.5	14.84	3.00	$H_2=10,$ $H_3=5.8$	$\rho_1=0.95,$ $\rho_2=1.65$	0.69
	4	0.5	17.83	3.00	$H_2=10,$ $H_3=5.1$	$\rho_1=0.95,$ $\rho_2=1.87$	0.92
	5	0.5	23.30	3.00	$H_2=10,$ $H_3=4.8$	$\rho_1=0.95,$ $\rho_2=1.99$	1.03
	6	0.5	26.22	3.00	$H_2=10,$ $H_3=4.6$	$\rho_1=0.95,$ $\rho_2=2.08$	1.12
Clay loam	1	0.5	04.58	3.14	$H_2=10,$ $H_3=7.5$	$\rho_1=1.00,$ $\rho_2=1.33$	0.33
	2	0.5	08.25	3.14	$H_2=10,$ $H_3=6.4$	$\rho_1=1.00,$ $\rho_2=1.56$	0.56
	3	0.5	12.48	3.14	$H_2=10,$ $H_3=5.5$	$\rho_1=1.00,$ $\rho_2=1.82$	0.82
	4	0.5	16.11	3.14	$H_2=10,$ $H_3=4.8$	$\rho_1=1.00,$ $\rho_2=2.08$	1.08
	5	0.5	20.58	3.14	$H_2=10,$ $H_3=4.7$	$\rho_1=1.00,$ $\rho_2=2.13$	1.13
	6	0.5	22.98	3.14	$H_2=10,$ $H_3=4.6$	$\rho_1=1.00,$ $\rho_2=2.17$	1.17
Loam	1	0.5	02.04	3.61	$H_2=10,$ $H_3=8.0$	$\rho_1=1.15,$ $\rho_2=1.44$	0.29

2.MATERIAL AND METHODS

	2	0.5	06.87	3.61	$H_2= 10,$ $H_3= 6.6$	$\rho_1 = 1.15,$ $\rho_2= 1.74$	0.59
	3	0.5	11.18	3.61	$H_2= 10,$ $H_3= 5.9$	$\rho_1 = 1.15,$ $\rho_2= 1.95$	0.80
	4	0.5	13.93	3.61	$H_2= 10,$ $H_3= 5.3$	$\rho_1 = 1.15,$ $\rho_2= 2.17$	1.02
	5	0.5	16.71	3.61	$H_2= 10,$ $H_3= 4.9$	$\rho_1 = 1.15,$ $\rho_2= 2.35$	1.20
	6	0.5	20.78	3.61	$H_2= 10,$ $H_3= 4.8$	$\rho_1 = 1.15,$ $\rho_2= 2.39$	1.24
	Loamy sand	1	0.5	01.25	4.21	$H_2= 10,$ $H_3= 7.9$	$\rho_1 = 1.34,$ $\rho_2= 1.70$
2		0.5	06.19	4.21	$H_2= 10,$ $H_3= 7.0$	$\rho_1 = 1.34,$ $\rho_2= 1.91$	0.57
3		0.5	08.21	4.21	$H_2= 10,$ $H_3= 6.7$	$\rho_1 = 1.34,$ $\rho_2= 2.00$	0.66
4		0.5	11.57	4.21	$H_2= 10,$ $H_3= 6.4$	$\rho_1 = 1.34,$ $\rho_2= 2.09$	0.75
5		0.5	14.30	4.21	$H_2= 10,$ $H_3= 6.1$	$\rho_1 = 1.34,$ $\rho_2= 2.20$	0.86
6		0.5	16.42	4.21	$H_2= 10,$ $H_3= 5.3$	$\rho_1 = 1.34,$ $\rho_2= 2.53$	1.19

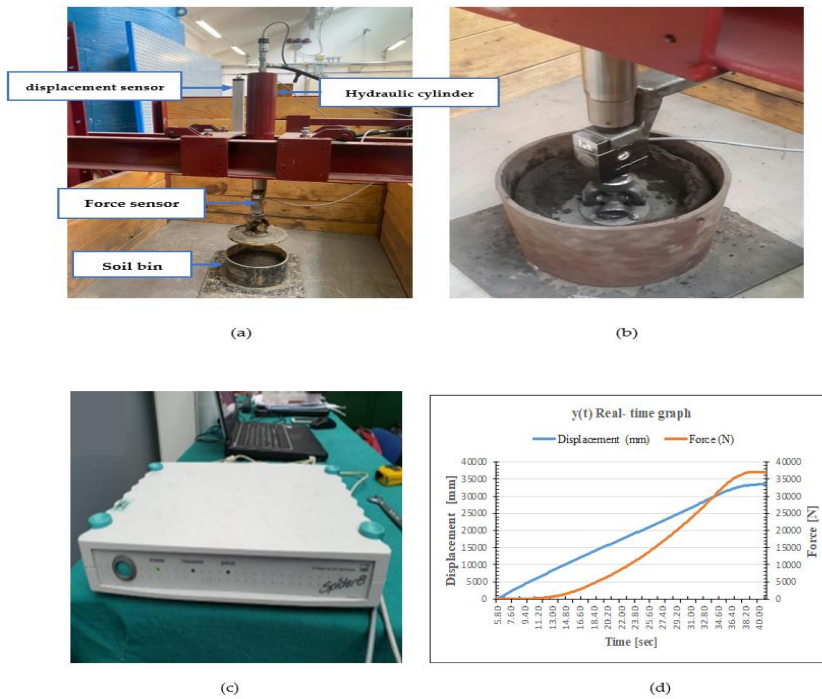


Figure 2.2. Shows (a) the main structure of the bevameter equipment, (b) the plate size, the soil bin, and the soil sample, (c) the data logger (Spider8), and (d) the CATMAN 4.5 software recording the data.

2.MATERIAL AND METHODS

3.2.2 Determining the moisture content of the soil

The Moisture Analyzer (HE53 230 V) was used to measure the soil's moisture content. It works based on the principle of drying. An amount of soil is placed on the tray inside the moisture analyzer, and the heating plates inside the moisture analyzer start to dry the sample till reaching an unchangeable soil mass (dry mass). Then calculates the moisture percentage by subtracting the remaining mass from the initial mass, and the answer is divided by the initial mass (the moisture content obtained is the wet-based result). The moisture analyzer is shown in Figures 2.3a, and Figure 2.3b.



Figure 2.3. The analyzer (a) shows the mass sample, and (b) shows the percentage of the moisture content.

3.2.3 Spectral behaviour measurements (colour test)

The Spectrophotometer CM-700d (see Figure 2.4a,2.4b) was used to measure the soil's colour (soil spectral behaviour). The colour of the soils was taken by the Spectrophotometer at each moisture content before the bevameter test.

The spectrophotometer sends electromagnetic waves in the visible range (400 – 700 nm; light visible band), and the colour of the soil will be determined based on the reflected wavelength (spectral reflectance %). Three records were taken by the spectrophotometer for the soil at each moisture content, and the averaging of these records was considered as the result.



Figure 2.4. Shows (a) the Spectrophotometer (CM-700d) and the 8mm head (the electromagnetic waves pass through), and (b) while measuring and recording the data.

3. RESULTS

This chapter presents the most important results obtained from the experimentation and their discussions.

3.1. Bevameter results (pressure-sinkage relationship)

The pressure-sinkage curves of the eight soils resulting from the bevameter test were read through the CATMAN 4.5 software (see Table 2). The results are shown in Figure 3.1. The rest of the results of the soils are provided in the dissertation.

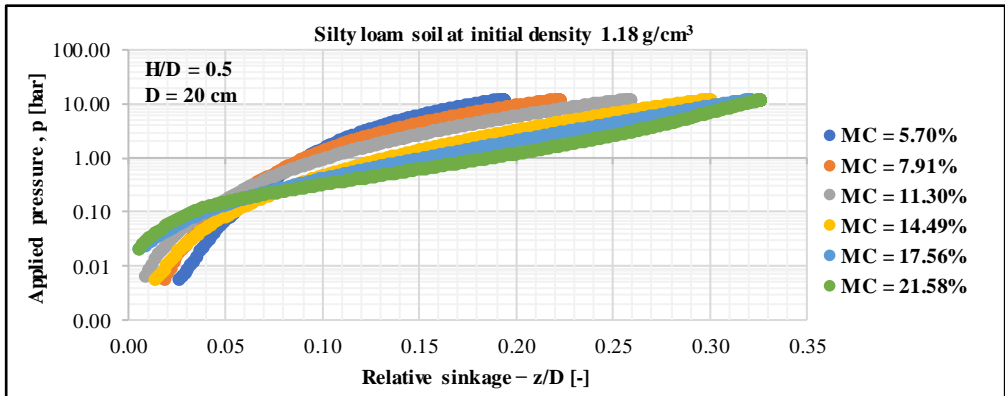


Figure 3.1. Silty loam soil texture pressure – sinkage relationship at different moisture contents for 1.18 g/cm³ density.

For every moisture content level, sinkage (expressed as the ratio z/D) escalates with the increase in applied pressure (the force divided by the plate's area). The pressure-sinkage relationship observed at each water content is consistent with the pressure-sinkage equation proposed by Saakyan in 1959, which is derived from the elastic half-space Boussinesq theory (referenced as Equation 3.1).

$$p = k \left(\frac{Z}{D} \right)^n \quad (3.1)$$

Where:

p : the applied pressure,

D : the diameter of the plate,

Z : the soil vertical deformation (sinkage),

k : the sinkage modulus.

n : exponent characterizes soil's deformation behaviour.

3.RESULTS

Equations 3.1 show that the sinkage is directly proportional to the pressure applied, as is evident in the resulting curves.

Under a constant applied pressure, sinkage is observed to increase with an increase in water level at varying moisture levels. The pressure-sinkage relationship traces a similar hyperbolic path across different moisture levels. At the peak applied pressure, approximately 12 bar, the greatest sinkage occurs at the highest moisture content, indicating that sinkage escalates with moisture increase at a set pressure.

3.2. The impact of moisture content

Soil moisture content significantly affects its compressibility, density, and load-bearing capacity. This section explores how varying moisture levels influence soil density and relative sinkage under uniform applied pressures.

3.2.1 On the soil density

The density of moist soil increases after compaction under a constant load. Higher moisture content makes the soil more compressible, leading to greater sinkage and increased density. Soil compressibility is analyzed by plotting the relative density ratio ($\Delta\rho$) against moisture content for the eight soil textures (see Figure 3.2), the rest of the results of the soils are provided in the dissertation. As moisture content increases, the relative density ratio also rises, as defined by Equation 3.2.

$$\Delta\rho = \frac{\rho_2 - \rho_1}{\rho_1} \quad (3.2)$$

3.2.2 On the soil relative sinkage

For the eight soil textures (see Figure 3.2), the rest of the results of the soils are provided in the dissertation. The relative sinkage (z/D) at an applied pressure of 1.0 bar is a function of moisture content. The results indicate that as moisture content increases, the sinkage rate also increases, demonstrating that elevated moisture levels generally lead to increased soil compaction under equivalent compressive loads. This aspect is critical in our research, as moisture significantly influences the bearing capacity of soil.

3.RESULTS

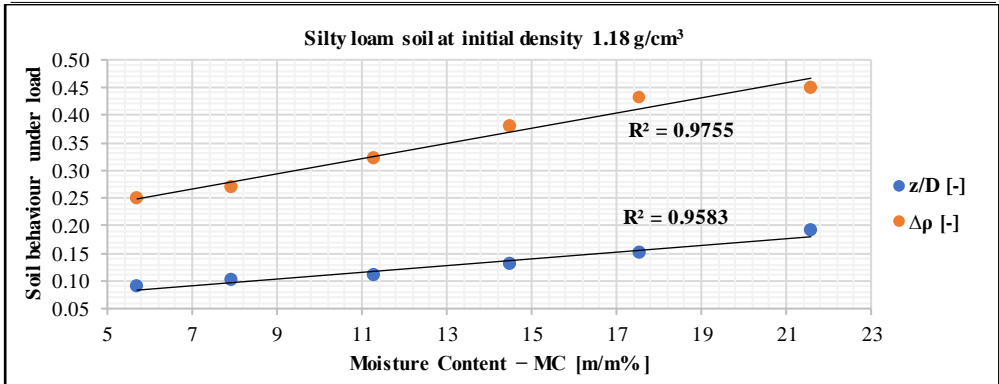


Figure 3.2. The relative sinkage and the relative density ratio for silty loam as a function of moisture content.

3.3. Spectral behaviour (Spectrophotometer)

For the eight soil samples, spectral behaviour was analysed using a spectrophotometer (Table 3.1, Figure 3.3), the rest of the results of the soils are provided in the dissertation. The spectral reflectance at each wavelength (400–700 nm) was derived from the curves. As incident wavelength increases, reflected wavelength also increases, regardless of moisture content.

With higher moisture content, reflected wavelength decreases at a fixed incident wavelength. At moisture levels below 550 nm, results overlap, showing that reflected wavelength stabilises in the 400–550 nm range. Thus, soil colour determination depends primarily on the 550–700 nm range.

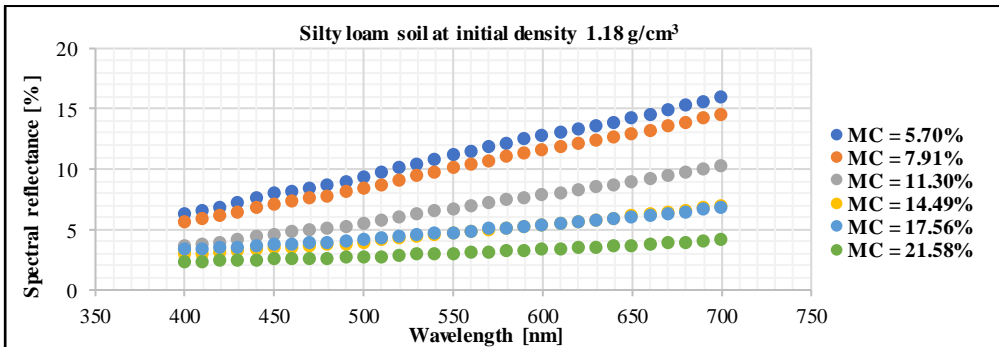


Figure 3.3. The spectral reflectance of silty loam soil in the visible range at varying moisture content levels.

3.3.1 Colour affected by moisture contents

To validate the findings presented in Figure 3.3, which demonstrate an inverse relationship between moisture content and soil reflectance, the reflection values were averaged across three spectral ranges: 400 – 500 nm, 400 – 700

3.RESULTS

nm, and 600-700 nm. Equations 3.3, 3.4, and 3.5 were employed to calculate the mean reflected wavelengths at varying moisture levels.

$$R_m^{4/5} = \frac{\sum_{400}^{500} R_i}{11} \quad (3.3)$$

$$R_m^{4/7} = \frac{\sum_{400}^{700} R_i}{31} \quad (3.4)$$

$$R_m^{6/7} = \frac{\sum_{600}^{700} R_i}{11} \quad (3.5)$$

Where:

R_i : The reflected wavelength at a specific spectrum of 400 – 700 nm.

$R_m^{4/5}$: The mean for wavelengths in the 400 – 500 nm range.

$R_m^{4/7}$: The mean for wavelengths in the 400 – 700 nm range.

$R_m^{6/7}$: The mean for wavelengths in the 600 – 700 nm range.

The Z (10°/D65) value, a spectrophotometer tristimulus parameter, decreases with increasing moisture, aligning with soil reflectance behaviour. Similarly, reflectance at 700 nm diminishes as moisture rises (Table 3.1). Figure 3.4 highlights the average reflectance (R_m) and values at 700 nm as moisture indicators. Table 3 summarizes average reflectance across 400–500 nm, 400–700 nm, and 600–700 nm, showing a consistent decrease with higher moisture levels. These findings demonstrate how moisture influences soil spectral properties, aiding in soil moisture estimation using spectral data.

Table 3.1. This table shows the main spectral reflectance parameters.

Soil texture	No.	MC [%]	Z(10°/D65)	$R_m^{(4/5)}$	$R_m^{(4/7)}$	$R_m^{(6/7)}$	Ref. at 700 nm
Sandy loam	1	01.12	07.60	06.98	09.81	12.54	14.30
	2	04.68	07.51	06.96	08.62	10.34	11.15
	3	08.77	06.55	06.07	07.47	08.88	09.49
	4	12.00	05.96	05.53	06.89	08.30	08.94
	5	15.04	05.95	05.50	06.90	08.28	08.80
	6	17.84	04.67	04.30	05.96	07.59	08.23
Silty loam	1	05.70	08.47	07.78	11.02	14.23	15.92
	2	07.91	07.58	06.96	09.96	12.92	14.49
	3	11.30	04.90	04.51	06.72	08.96	10.24
	4	14.49	03.67	03.39	04.71	06.09	06.94
	5	17.56	03.97	03.68	04.80	06.00	06.79
	6	21.58	02.66	02.46	03.03	03.64	04.06
Clay	1	10.23	09.49	08.75	12.47	16.41	18.81
	2	14.40	07.57	06.99	09.94	13.12	15.16
	3	17.00	05.81	05.38	07.19	09.19	10.57
	4	21.58	05.41	05.00	06.52	08.15	09.20
	5	24.19	05.53	05.12	06.40	07.80	08.75

3.RESULTS

	6	26.73	05.14	04.77	05.77	06.87	07.62
Sand	1	01.09	08.67	07.97	12.26	16.64	18.97
	2	03.90	06.47	05.95	09.26	12.70	14.59
	3	06.74	05.90	05.43	08.32	11.32	12.94
	4	09.37	06.42	05.91	08.46	11.09	12.49
	5	12.19	06.08	05.59	08.21	10.92	12.39
	6	15.08	05.69	05.23	07.61	10.07	11.36
Silty clay	1	04.02	08.68	08.02	10.67	13.40	15.10
	2	10.69	07.96	07.36	09.76	12.24	13.80
	3	14.84	06.18	05.71	07.79	10.00	11.49
	4	17.83	04.93	04.57	06.05	07.68	08.88
	5	23.30	04.84	04.49	05.52	06.66	07.52
	6	26.22	04.16	03.87	04.76	05.79	06.63
Clay loam	1	04.58	06.44	05.92	08.93	12.05	13.66
	2	08.25	05.88	05.40	08.24	11.21	12.99
	3	12.48	05.42	04.99	07.87	10.96	12.80
	4	16.11	04.86	04.49	06.76	09.23	10.74
	5	20.58	04.65	04.29	05.93	07.69	08.69
	6	22.98	04.22	03.89	05.54	07.32	08.38
Loam	1	02.04	14.83	12.77	19.91	26.68	28.48
	2	06.87	13.96	13.59	20.39	26.78	28.33
	3	11.18	11.17	10.22	17.06	23.69	25.63
	4	13.93	08.47	07.72	13.20	18.35	19.43
	5	16.71	08.52	07.77	12.94	17.81	18.83
	6	20.78	07.47	06.86	11.39	15.84	17.11
Loamy sand	1	01.25	06.96	06.42	09.88	13.54	15.47
	2	06.19	04.98	04.62	07.34	10.41	12.27
	3	08.21	04.43	04.10	05.89	07.89	09.12
	4	11.57	05.24	04.85	06.35	08.00	08.94
	5	14.30	05.97	05.51	06.96	08.48	09.23
	6	16.42	04.93	04.54	06.35	08.27	09.25

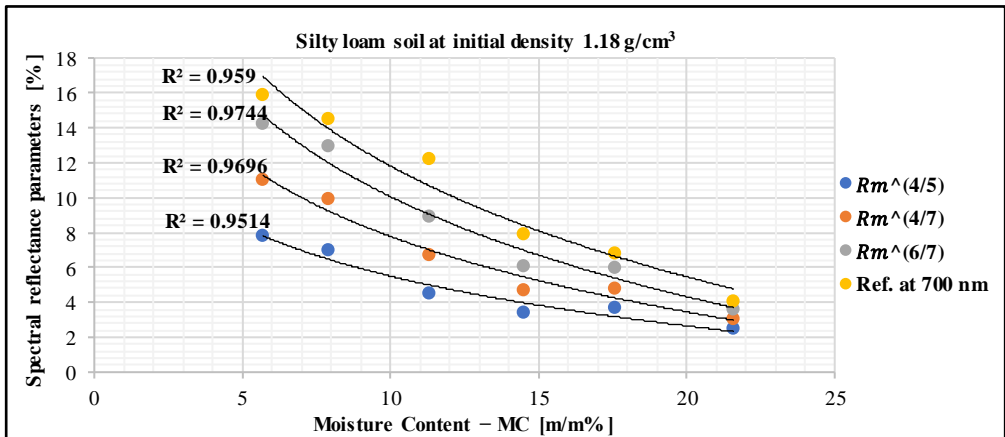


Figure 3.4. Spectral reflectance parameter – moisture content relationship for silty loam.

Based on the analysis of Table 3.1 and Figure 3.4, it can be concluded that the reflectance at 700 nm exhibits greater sensitivity to moisture content and warrants consideration when evaluating spectral reflectance.

3.RESULTS

3.4.Soil properties underload and the spectral reflectance at 700 nm

3.4.1 Soil relative density ratio – reflectance at 700 nm relationship

Based on the results (see Figure 3.5), the relationship between the reflectance at 700 nm and the soil density ratio demonstrates that an increase in reflectance corresponds to a decrease in the soil density ratio. Consequently, this correlation indicates a reduction in sinkage (signifying high load-bearing capacity) and vice versa.

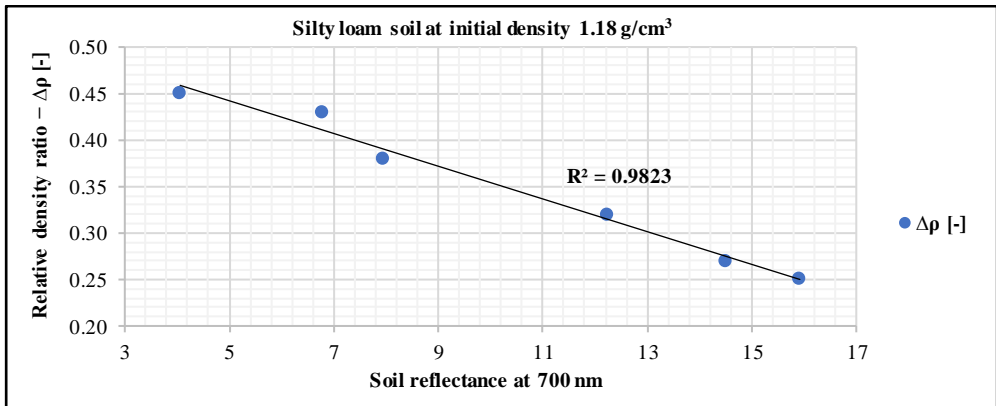


Figure 3.5. Soil relative density ratio – Spectral reflectance at 700 nm relationship for silty loam.

3.4.2 Soil relative sinkage – spectral reflectance at 700 nm relationship

The relationship between the reflectance at 700 nm and the soil's relative sinkage, as illustrated in Figure 3.6, demonstrates that an increase in reflectance corresponds to a decrease in the soil's relative sinkage. Consequently, this indicates a reduction in sinkage (signifying the high load-bearing capacity) and vice versa.

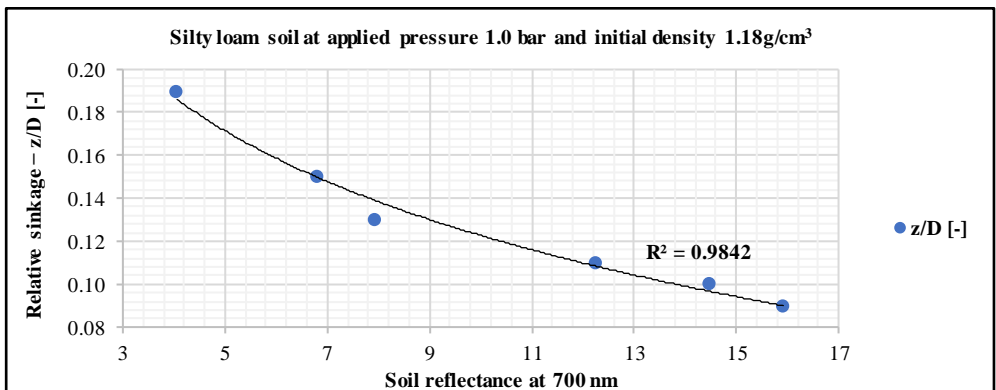


Figure 3.6. Soil relative sinkage – Spectral reflectance at 700 nm relationship for silty loam.

3.RESULTS

3.5. Estimation of soil-specific constants and moisture content

The soil samples were oven-dried at 105°C for 24 hours to achieve near-zero moisture content. The objective was to determine the values of constants \hat{A} and \hat{n} for each soil type, as outlined in Table 3.2. These values were used to calculate the reference reflectance using Equation 3.6. With established, we applied equation 3.7 to estimate the moisture content for each soil sample.

$$R_{MC\%}^{700} = R_{0\%}^{700} - \hat{A} \cdot MC\%^{\hat{n}} \quad (3.6)$$

$$MC\% = \sqrt[\hat{n}]{\frac{R_{0\%}^{700} - R_{MC\%}^{700}}{\hat{A}}} \quad (3.7)$$

The soil spectral behaviour at 700 nm with the moisture content for silty loam soil textures, as in Figure 3.7 (The rest of the results of seven soil textures are provided in the dissertation). The curves were made using Equation 3.6.

Table 3.3 Values of the constants for Equations (3.6) and (3.7)

Soil texture	\hat{A} [-]	\hat{n} [-]	$R_{0\%}^{700}$ [%]
Sandy loam	1.20	0.84	14.30
Silty loam	0.37	0.85	12.20
Clay	0.41	0.83	15.80
Sand	0.66	0.83	17.50
Silty clay	0.57	0.84	18.40
Clay loam	0.55	0.83	19.70
Loam	0.85	0.79	20.50
Loamy sand	0.56	0.83	34.40

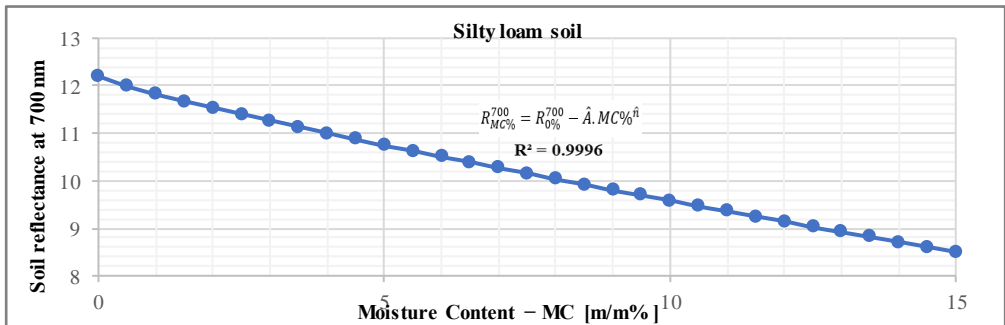


Figure 3.7. Spectral reflectance at 700 nm – soil moisture content relationship for silty loam.

3.6. Soil load bearing capacity – optical reflectance relationship

At the beginning of the compaction, there is a small transient phenomenon when the soil conforms to the pressure plate and settles. Based on the measurements, this ends at approximately $z/D = 0.05$ and from there the curve

3.RESULTS

follows according to the discovered function. This will be the starting point of the curve.

$$p_0 = k_0 \cdot \left(\frac{z_0}{D}\right)^n \quad (3.8)$$

where:

n=0.8 for sandy loam,

Substituting the given values:

$$p_0 = k_0 \cdot 0.1 \quad (3.9)$$

The change in soil pressure under the plate is given by:

$$\Delta p = p_0 - p \quad (3.10)$$

Rearranging for p:

$$p = p_0 - \Delta p \quad (3.11)$$

The pressure difference due to moisture content (MC%) is:

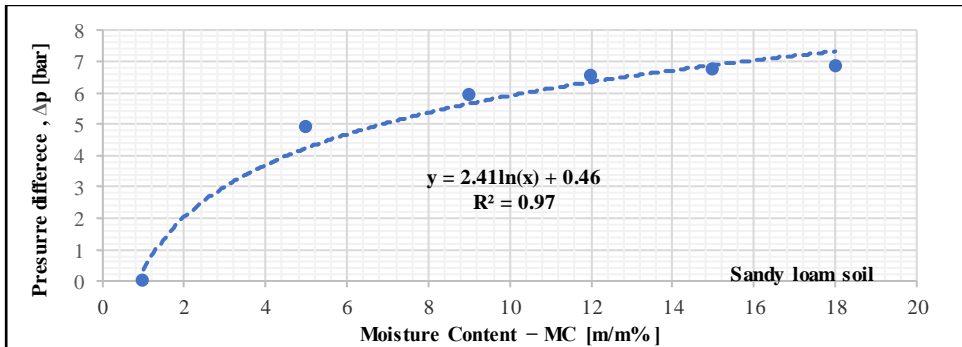


Figure 3.8. Pressure difference – soil moisture content relationship for sandy loam.

$$\Delta p = 2.41 \cdot \ln(MC\%) + 0.46 \quad (3.12)$$

Since the moisture content is related to spectral reflectance by:

$$MC\% = \left(\frac{R_{0\%}^{700} - R_{MC\%}^{700}}{2.75} \right)^{\frac{1}{0.35}} \quad (3.13)$$

Substituting (3.13) into (3.12) and into the pressure equation (3.11):

3.RESULTS

$$p = k_0 \cdot 0.1 - 2.41 \cdot \ln \left[\left(\frac{R_{0\%}^{700} - R_{MC\%}^{700}}{2.75} \right)^{\frac{1}{0.35}} \right] + 0.46 \quad (3.14)$$

We add one to the input variable of the ln function so that it will be valid from zero.

Thus, the corrected equation for load-bearing capacity is:

$$p = k_0 \cdot 0.1 - 2.41 \cdot \ln \left[1 + \left(\frac{R_{0\%}^{700} - R_{MC\%}^{700}}{2.75} \right)^{\frac{1}{0.35}} \right] + 0.46 \quad (3.15)$$

The final formulation:

$$p = a \cdot k_0 - c - f \cdot \ln \left[1 + \left(\frac{R_{0\%}^{700} - R_{MC\%}^{700}}{\hat{A}} \right)^{\frac{1}{\hat{n}}} \right] \quad (3.16)$$

where a, c, f, \hat{A} , and \hat{n} are empirical constants dependent on soil texture and spectral properties. During validation, it was revealed that c is a negative constant. We take this into account in the equation.

3.7. Soil saturation- spectral reflectance relationship

This study investigated sand and loamy sand soil, utilizing known reflectance parameters of dry soil and saturated soil, and employing the saturation " ε " with the following equation, where " R_{Sat}^{700} " represents the reflectance of fully saturated soil:

$$\varepsilon = \frac{R_0^{700} - R^{700}}{R_0^{700} - R_{Sat}^{700}} \quad (3.17)$$

The higher saturation values observed in the sand indicate a more substantial reduction in reflectance when saturated, which is indicative of its rapid drainage and lower water retention capacity. Loamy sand exhibited lower saturation values, suggesting a more stable reflectance due to its finer texture and enhanced moisture retention properties (Table 3.4).

Table 3.4. Shows the data of soil textures investigated as follows:

Soil texture	Dry	Fully saturated		Reflectance range	Soil particle distribution		
	R_0^{700} [%]	R_{Sat}^{700} [%]	MC_{Sat} [m/m%]	ΔR_{Max}	Clay [%]	Silt [%]	Sand [%]
Sand	17.30	06.86	30.00	10.40	02.20	02.10	95.70
Sandy loam	14.30	08.20	35.00	06.10	05.80	12.10	82.10

3.RESULTS

3.8.The effect of the load velocity on the soil sinkage

A significant correlation between load velocity and soil sinkage was observed when examining the load-bearing capacity of a homogeneous soil layer under varying velocities. Higher velocities resulted in reduced sinkage, while lower velocities led to increased sinkage due to the soil's mechanical response to loading rates. At lower velocities, the soil had more time to compact, increasing density and resistance to deformation, whereas rapid load application limited compaction, reducing sinkage. These findings align with terramechanics principles, where soil response depends on time, pressure, and material properties. Increased sinkage at slower velocities may result from the soil's ability to redistribute particles, forming a denser layer, while rapid loading restricts this rearrangement. Understanding this velocity-soil deformation relationship is essential for optimizing off-road vehicle design and soil interaction models across diverse terrains and load conditions. Further analysis of soil texture, moisture content, and particle size distribution could enhance insights into this behaviour.

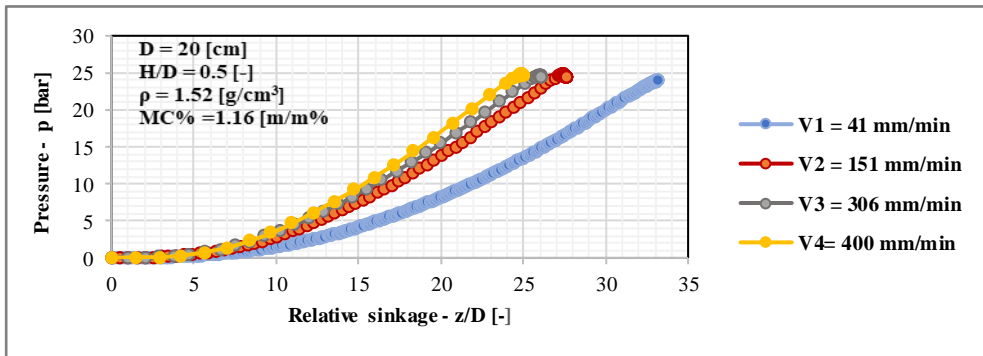


Figure 3.9. The load velocity affects the sinkage of sandy loam soil.

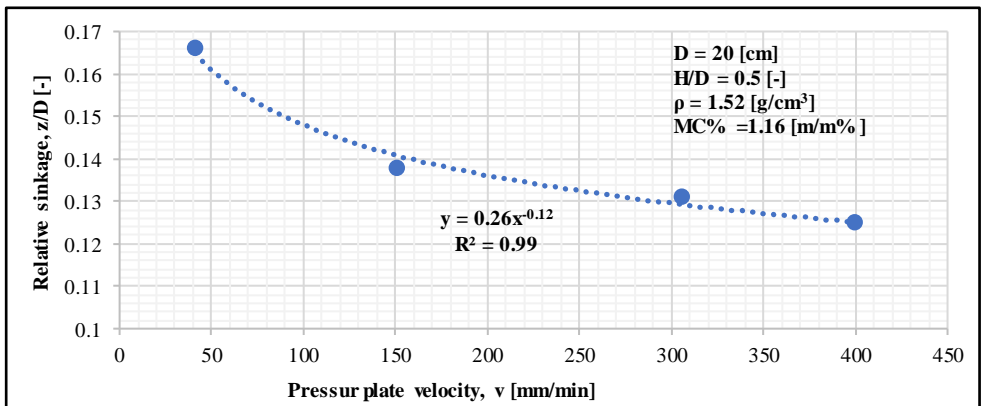


Figure 3.10. The sinkage as a function of velocity for sandy loam soil.

4. NEW SCIENTIFIC RESULTS

This section presents the new scientific findings from the research work as follows:

1. Soil saturation- spectral reflectance relationship

I investigated sand and sandy loam soil, knowing the reflectance parameters of dry soil and saturated soil, the saturating level " ε " can be calculated by the following equation, where " R_{Sat}^{700} " is the reflectance of fully saturated soil, " R_0^{700} " is the reflectance of the dry soil and the " R^{700} " is the measured reflectance:

$$\varepsilon = \frac{R_0^{700} - R^{700}}{R_0^{700} - R_{Sat}^{700}}$$

Traditional methods for measuring soil saturation rely on collecting physical samples and conducting laboratory analyses. In contrast, this method utilizes reflectance measurements, enabling field-based assessments of soil water saturation without the need for sample collection. By first obtaining reflectance measurements for both fully saturated and completely dry soil, subsequent reflectance readings can be used to calculate the current saturation level of the soil. This approach offers a more efficient and convenient way to monitor soil moisture conditions in agricultural settings.

Data of soil textures investigated are listed as follows:

Soil texture	Dry	Fully saturated		Reflectance range	Soil particle distribution		
	R_0^{700} [%]	R_{Sat}^{700} [%]	MC _{Sat} [m/m %]	ΔR_{Max}	Clay [%]	Silt [%]	Sand [%]
Sand	17.30	06.86	30.00	10.40	02.20	02.10	95.70
Sandy loam	14.30	08.20	35.00	06.10	05.80	12.10	82.10

2. Soil moisture content from soil spectral reflectance

At a 700 nm wavelength, I found a correlation between soil surface moisture content and measured reflectance. Calculating moisture content using this correlation requires knowing three constants specific to the soil texture, including the reflectance of the dry soil at 700 nm. These constants for each analyzed soil texture are presented in the table below.

$$MC\% = \sqrt{\frac{\hat{n} (R_{0\%}^{700} - R_{MC\%}^{700})}{\hat{A}}}$$

The value of the constants is as follows:

Soil texture	\hat{A} [-]	\hat{n} [-]	$R_{0\%}^{700}$ [%]
Sandy loam	1.20	0.84	14.30

4. NEW SCIENTIFIC RESULTS

Silty loam	0.37	0.85	12.20
Clay	0.41	0.83	15.80
Sand	0.66	0.83	17.50
Silty clay	0.57	0.84	18.40
Clay loam	0.55	0.83	19.70
Loam	0.85	0.79	20.50
Loamy sand	0.56	0.83	34.40

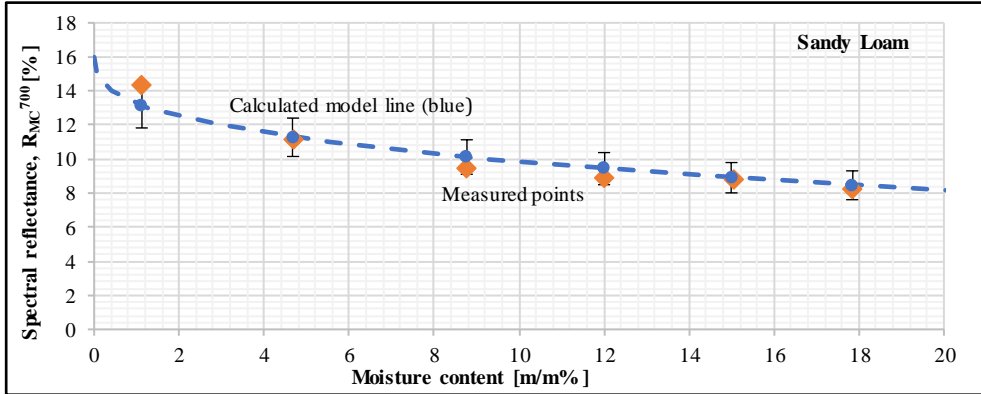


Figure 4.1. Model accuracy for sandy loam soil.

3. The load-bearing capacity and the spectral behaviour of soil relationship

For a homogeneous soil volume under confined compression with a H/D ratio of 0.5, I established a relationship between the soil's surface reflectance at 700 nm and its load-bearing capacity (p , [bar]). This relationship incorporates specific constants listed in the diagram. Furthermore, the equation contains the load-bearing capacity factor (k_0 , [bar]) at a relative sinkage (z/D , [-]) of 0.05 in a dry state, and the reflectance of dry soil (R_0^{700} , [%]) at 700 nm. The reflectance of the soil at 700 nm with a given moisture content ($R_{MC\%}^{700}$, [%]) serves as the independent variable.

$$p = a \cdot k_0 - c - f \cdot \ln \left[1 + \left(\frac{R_0^{700} - R_{MC\%}^{700}}{\hat{A}} \right)^{\frac{1}{\hat{n}}} \right]$$

The validity limit is the reflectance of dry soil to saturated soil. For sandy loam 14.3-8.2%

4. NEW SCIENTIFIC RESULTS

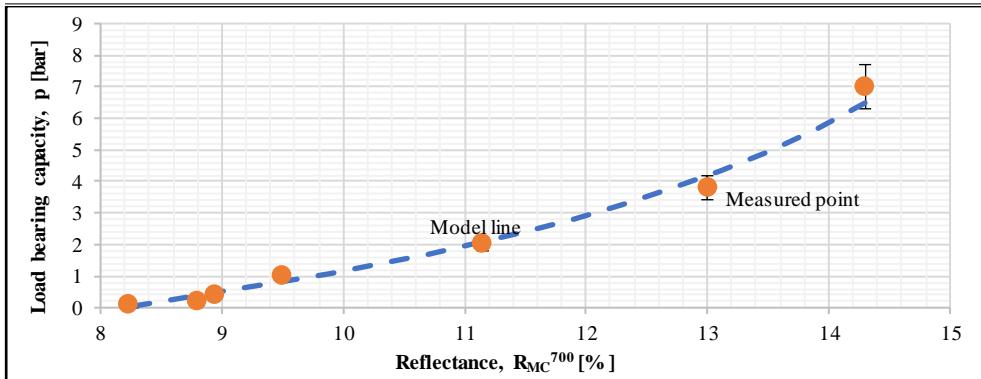


Figure 4.2. Reflectance-load bearing capacity relationship for sandy loam.

4. Pressure plate displacement as a function of its velocity

Under the conditions illustrated in the diagram, I determined a power function relationship between the pressure plate's velocity (rate of descent) and its sinkage. This relationship is expressed with two dimensionless constants, A and b, that include the effect of the soil properties and its initial condition. Further incorporates the plate diameter (D) and its velocity (v) as independent variables. The validity range of the equation for the velocity is between 40-400 mm/min.

$$z = D \cdot A \cdot v^{-b}$$

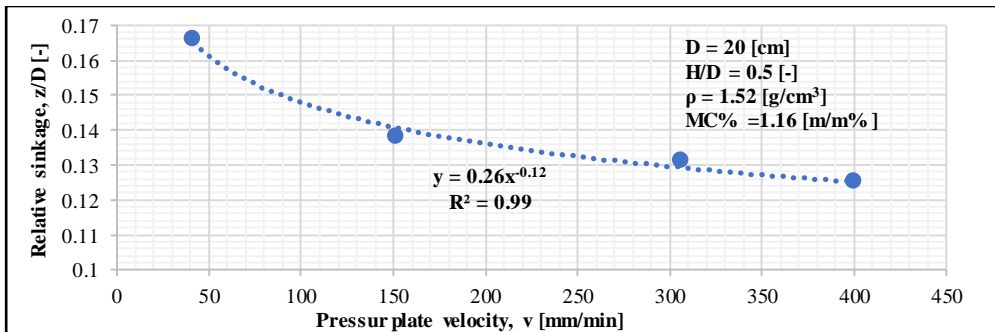


Figure 4.3. The relative sinkage as a function of the pressure plate's velocity.

5. Soil relative sinkage – moisture content relationship

Based on the measured data, I developed a new equation to determine the relative sinkage (z/D). This equation is valid for the given initial density as a function of moisture content, where A_1 and B_1 are constants depending on the soil texture. They are listed in the table below for different soil textures at 1.0 bar tyre inflation pressure, which is commonly utilized in agriculture applications.

$$z/D = A_1 \cdot MC\% + B_1$$

4. NEW SCIENTIFIC RESULTS

Soil texture	A_1 [-]	B_1 [-]	Regression, R2	MC[m/m%]
Sandy loam	0.0072	0.0404	0.9647	01 – 16
Silty loam	0.0061	0.0488	0.9583	01 – 22
Clay	0.0096	0.0154	0.9764	10 – 27
Sand	0.0053	0.0437	0.9798	01 – 16
Silty clay	0.0084	0.0208	0.9720	04 – 27
Clay loam	0.0106	0.0139	0.9919	04 – 23
Loam	0.0125	0.0208	0.9510	02 – 21
Loamy sand	0.0105	0.0710	0.9654	01 – 17

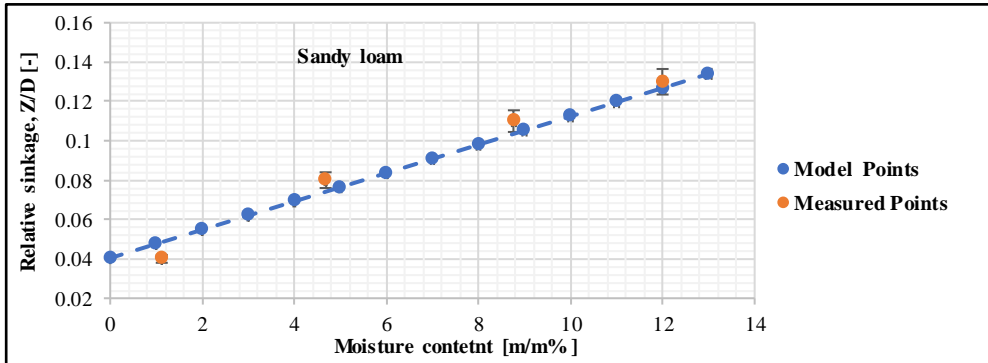


Figure 4.4. Soil relative sinkage – moisture content relationship for sandy loam.

6. Soil relative sinkage – spectral reflectance relationship

I experimentally determined and measured the soil spectral behaviour and load-bearing capacity (pressure-sinkage relationship) simultaneously under controlled moisture content conditions. Based on the experimental results, I focused on soil reflectance at 700 nm in relation to soil relative sinkage (z/D) under an applied pressure of 1.0 bar, corresponding to the typical tyre inflation pressure in vehicle mobility, as a function of moisture content. Through the analysis of graphs derived from the experiments, I experimentally revealed that soil spectral reflectance is inversely proportional to soil relative sinkage (z/D). Consequently, I developed a novel equation to determine the relative sinkage as a function of soil reflectance at 700 nm, where A_2 and B_2 are constants dependent on soil texture and soil spectral reflectance, as presented in the table below:

$$z/D = -A_2 \cdot \ln (R_{MC\%}^{700}) + B_2$$

Soil texture	A_2 [-]	B_2 [-]	Regression, R2	MC[m/m%]
Sandy loam	0.211	0.5921	0.9825	01 – 16
Silty loam	0.071	0.2845	0.9842	01 – 22
Clay	0.162	0.5558	0.8720	10 – 27
Sand	0.218	0.6499	0.9326	01 – 16
Silty clay	0.208	0.6372	0.9879	04 – 27
Clay loam	0.376	1.0693	0.9788	04 – 23
Loam	0.455	1.5836	0.9980	02 – 21
Loamy sand	0.231	0.7096	0.9768	01 – 17

4.NEW SCIENTIFIC RESULTS

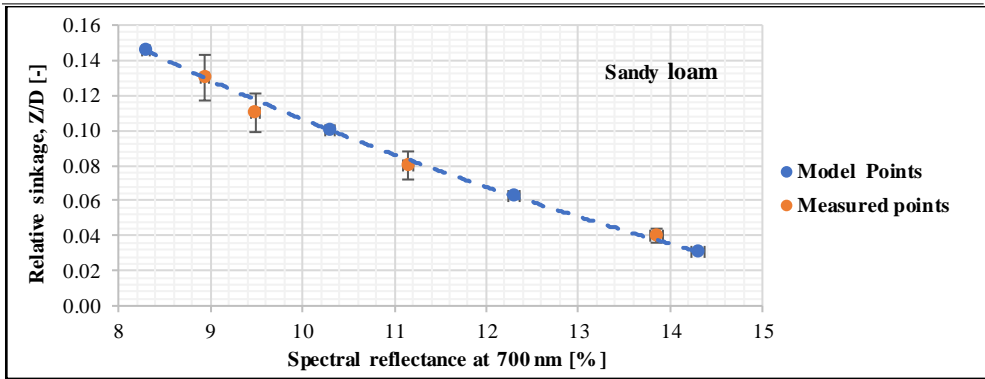


Figure 4.5. Soil relative sinkage – spectral reflectance relationship for sandy loam.

5. CONCLUSION AND SUGGESTIONS

In conclusion, experimental analysis studied the load-bearing capacity and spectral behaviour of eight homogenous soil textures. The load-bearing capacity is represented by the pressure-sinkage relationship. A bevameter apparatus examined load-bearing capacity and soil properties via normal load applied to the soil surface. Experiments used a circular sinkage plate (20 cm) with soil thickness (10 cm). Applied force, time and plate displacement were recorded by Catman4.5 software through Spider8. These data determined the applied pressure (p) and relative sinkage (z/D) relationship at different moisture content levels. Pressure–sinkage curves were plotted using a logarithmic scale. Densities before and after measurement along with soil mass were identified to calculate the relative density ratio ($\Delta\rho$). For spectral behaviour, soil reflectance was measured for the same sample prepared for the bevameter technique. Based on measurements and findings, it is possible to make the following inferences:

- The pressure-sinkage relationship for eight soil textures showed that relative sinkage (z/D) increases proportionally with applied pressure and relative density ratio ($\Delta\rho$) at varying moisture content levels.
- Spectral reflectance curves revealed that reflected wavelengths increased with sent wavelengths at the same moisture content. However, higher moisture content at a fixed sent wavelength reduced reflectance.
- Reflectance calculations for 700 nm, 400–500 nm, 400–700 nm, and 600–700 nm ranges indicated that 700 nm reflectance is highly sensitive to moisture content, making it crucial for spectral evaluations.
- The experiment established a link between soil properties (relative sinkage, relative density ratio) through the moisture content and spectral reflectance at 700 nm.
- identifying reflectance parameters for dry and saturated sand and loamy sand soils. These parameters enable the determination of soil saturation and moisture levels.
- Near-zero moisture content tests confirmed that soil reflectance parameters can reliably indicate moisture content.

As a suggestion, additional experiments should be performed with inhomogeneous soil samples, first in laboratory environments and then in the field. These studies should seek to confirm the newly proposed correlations between load-bearing capacity and moisture levels, as well as between load-bearing capacity and spectral characteristics. Moreover, these investigations should strive to verify the generalised relationship linking load-bearing capacity to spectral reflectance.

6. SUMMARY

INFLUENCE OF MOISTURE CONTENT ON SOIL BEARING CAPACITY AND SPECTRAL REFLECTANCE

This study conducted experiments to establish the relationship between load-bearing capacity and soil colour across eight soil textures. Soil samples from various locations in Hungary were tested as homogeneous. The bevameter apparatus measured load-bearing capacity, while a spectrophotometer assessed spectral reflectance (soil colour). Both properties were measured under controlled conditions, maintaining constants such as moisture content, initial density, and a H/D ratio of 0.5.

The bevameter tests identified the relative density ratio and relative sinkage at various moisture levels, while the spectrophotometer assessed soil reflectance under different moisture conditions. Results from both tests were categorized into:

1. A novel equation for determining the relative sinkage (z/D) was developed based on experimental results, as a function of moisture content.
2. A relationship of the relative soil density ratio ($\Delta\rho$) was found based on these experimental results.
3. A novel relationship concerning the relative sinkage (z/D) with the soil reflectance at 700 nm was proposed based on experimental results.
4. Additionally, a new relationship of the relative soil density ratio ($\Delta\rho$) with the soil reflectance at 700 nm was proposed.
5. Soil saturation-reflectance was investigated for sand and loamy sand soil, considering the reflectance parameters of dry soil and saturated soil.
6. A new moisture content equation (MC%) derived from the soil spectral reflectance has been proposed based on the experimental results.
7. It was concluded that the reflectance at 700 nm exhibits greater sensitivity to moisture content and should be considered when evaluating spectral reflectance.
8. A novel equation developed for determining the sinkage as a function of the velocity for sandy loam soil.
9. A novel equation was developed to determine the relationship between the load-bearing capacity and the soil spectral reflectance, based on experimental results, as a function of moisture content.

As a recommendation, further experimental investigations should be conducted with inhomogeneous soil, initially in laboratory settings and subsequently in field conditions, to validate the proposed new relationships between load-bearing capacity and moisture content, as well as between load-bearing capacity and colour.

7. MOST IMPORTANT PUBLICATIONS RELATED TO THE THESIS

Referred papers in foreign languages:

1. **Ahmed A.E.E.**, El Hariri A., Kiss P., (2023): Soil Spectral Behavior Related to Its Load-Bearing Capacity Based on Moisture Content. Applied Sciences. 13(6):3498. <https://doi.org/10.3390/app13063498> (Q2)
2. El Hariri A., **Ahmed A. E. E.**, Kiss P., (2023): Review on soil shear strength with loam sand soil results using direct shear test, Journal of Terramechanics, vol. 107, Pp.47-59, ISSN 0022-4898, <https://doi.org/10.1016/j.jterra.2023.03.003>. (Q1)
3. Pillinger G., **Ahmed E.E.A.**, Kornél B., Kiss P., (2023): Correlations between moisture content and colour spectrum of sandy soils, Journal of Terramechanics, vol.108, Pp. 39-45, ISSN 0022-4898, <https://doi.org/10.1016/j.jterra.2023.05.002> (Q1)
4. El Hariri A., **Ahmed A.E.E.**, Kiss P., (2023): Sandy Loam Soil Shear Strength Parameters and Its Colour. Applied Sciences. 2023; 13(6):3847. <https://doi.org/10.3390/app13063847> (Q2)
5. **Ahmed E. E. A.**, Pillinger G., Kiss P., (2022): The influence of sandy loam soil moisture content on its load-bearing capacity, Mechanical Engineering Letters, Gödöllő, Hungary, 2021, Vol. 22, Pp.15-25. HU ISSN 2060-3789.
6. **Ahmed A.E.E.**, El Hariri A., Kiss P., (2021): Soil strength and load bearing capacity measurement techniques. Hungarian Agricultural Engineering (40). pp. 16-27. ISSN 0864-7410 <https://doi.org/10.17676/HAE.2021.40.164>
7. MohammedZein, M. A., Michéli, E., Rotich, B., Justine, P. N., **Ahmed, A. E. E.**, Tharwat, H., Csorba, Á. (2023): Rapid Detection of Soil Texture Attribute based on Mid-Infrared Spectral Library In Salt Affected Soils of Hungary. Hungarian Agricultural Engineering (42). Pp. 5-13. ISSN 0864-7410 (print); 2415-9751 <https://doi.org/10.17676/HAE.2023.42.5>
8. **Ahmed A. E. E.**, Pillinger G., Kiss P., (2025). The Connection of Sandy Loam Soil Moisture Content to the Load-Bearing Capacity. Ingeria automobilului, (x), xx-xx. ISSN xxxx – xxxx <https://siar.ro/publicatii/> (accepted)

Refereed papers in Hungarian:

9. **Ahmed E.E.A.**, Kiss P., (2022): Homokos Vályogtalaj Teherbíróképességének Yizsgálata Bevaméterrel, Mezőgazdasági Technika, ISSN 0026-1890 : 63 (6), pp 2-6

International conference proceedings:

10. **Ahmed E. E. A.**, Pillinger G., Kiss P., (2023): Moisture content impacts on

soil load bearing capacity and its spectral behaviour. 16th European-African Regional Conference of the ISTVS, Lublin, Poland, October 11-13, 2023, <https://doi.org/10.56884/DTUX6735>

11. Pillinger G., **Ahmed E. E. A.**, Kiss P., (2024): Effect of initial soil colour on sandy soil moisture content determination, 21st International and 12th Asia-Pacific Regional Conference of the ISTVS, Yokohama, Japan, October 28-31, 2024, <https://doi.org/10.56884/GV41C6MW>

International conference abstracts:

12. **Ahmed E. E. A.**, Pillinger G., Kiss P., (2024): Investigating the spectral behaviour and load bearing of soil, In Bakacsi, Zsófia; Horel, Ágota; Mészáros, János; Rékási, Márk; Takács, Tünde (eds.), Alternatives to Reduce Soil Degradation (ARSD2024) - Book of abstracts, Conference: Budapest, Hungary 2024.05.07., -2024.05.07. Bp: HUN-REN Centre for Agricultural Research, Vol. 62, Pp. 35-35, ISBN: 9786155387128
13. **Ahmed E. E. A.**, Pillinger G., Kiss P., (2024): Correlation Between Soil Moisture, Spectral Response, and Load Capacity, In Annual Conference 2024 Abstract Book: British Society of Soil Science (BSSS) (2024) 115 p. pp. 107-107. , 1 p.